Real-Time and Embedded Systems Lab (mLAB)   School of Engineering and Applied Science

4-2014

Model-IQ: Uncertainty Propagation from Sensing to Modeling and Control in Buildings.

Madhur Behl
University of Pennsylvania, mbehl@seas.upenn.edu

Truong Nghiem
University of Pennsylvania, nghiem@seas.upenn.edu

Rahul Mangharam
University of Pennsylvania, rahulm@seas.upenn.edu

Model-IQ: Uncertainty Propagation from Sensing to Modeling and Control in Buildings.

Abstract

A fundamental problem in the design of closed-loop Cyber-Physical Systems (CPS) is in accurately capturing the dynamics of the underlying physical system. To provide optimal control for such closed-loop systems, model-based controls require accurate physical plant models. It is hard to analytically establish (a) how data quality from sensors affects model accuracy, and consequently, (b) the effect of model accuracy on the operational cost of model-based controllers. We present the Model-IQ toolbox which, given a plant model and real input data, automatically evaluates the effect of this uncertainty propagation from sensor data to model accuracy to controller performance. We apply the Model-IQ uncertainty analysis for model-based controls in buildings to demonstrate the cost-benefit of adding temporary sensors to capture a building model. We show how sensor placement and density bias training data. For the real building considered, a bias of 1% degrades model accuracy by 20%. Model-IQ's automated process lowers the cost of sensor deployment, model training and evaluation of advanced controls for small and medium sized buildings. Such end-to-end analysis of uncertainty propagation has the potential to lower the cost for CPS with closed-loop model based control. We demonstrate this with real building data in the Department of Energy's HUB.

Keywords

modeliq, inverse modeling, building modeling, energy-efficient control, uncertainty, mpc, model predictive control, sensing, retrofitting

Disciplines

Computer Engineering | Electrical and Computer Engineering | Systems Engineering

Comments

@article{behl_iccps14,

author = {Madhur Behl, Truong Nghiem and Rahul Mangharam},

title = {Model-IQ: Uncertainty Propagation from Sensing to Modeling and Control in Buildings},

journal = {ACM/IEEE International Conference on Cyber-Physical Systems},

year = {2014}

}

Model-IQ: Uncertainty Propagation from Sensing to Modeling and Control in Buildings

Madhur Behl, Truong X. Nghiem and Rahul Mangharam
Dept. of Electrical and Systems Engineering, University of Pennsylvania
Philadelphia, USA
(mbehl,nghiem,rahulm)@seas.upenn.edu

ABSTRACT

A fundamental problem in the design of closed-loop Cyber-Physical Systems (CPS) is in accurately capturing the dynamics of the underlying physical system. To provide optimal control for such closed-loop systems, model-based controls require accurate physical plant models. It is hard to analytically establish (a) how data quality from sensors affects model accuracy, and consequently, (b) the effect of model accuracy on the operational cost of model-based controllers. We present the Model-IQ toolbox which, given a plant model and real input data, automatically evaluates the effect of this uncertainty propagation from sensor data to model accuracy to controller performance. We apply the Model-IQ uncertainty analysis for model-based controls in buildings to demonstrate the cost-benefit of adding temporary sensors to capture a building model. We show how sensor placement and density bias training data. For the real building considered, a bias of 1% degrades model accuracy by 20%. Model-IQ's automated process lowers the cost of sensor deployment, model training and evaluation of advanced controls for small and medium sized buildings. Such end-to-end analysis of uncertainty propagation has the potential to lower the cost for CPS with closed-loop model based control. We demonstrate this with real building data in the Department of Energy's HUB.

Categories and Subject Descriptors: D.4.8 [Performance]: Modeling and prediction—*energy-efficient buildings*

1. INTRODUCTION

One of the biggest challenges in the domain of cyber physical energy systems is in accurately capturing the dynamics of the underlying physical system. In the context of buildings, the modeling difficulty arises due to the fact that each building is designed and used in a different way and therefore, it has to be uniquely modeled. Furthermore, each building system consists of a large number of interconnected subsystems which interact in a complex manner and are subjected to time varying environmental conditions.

Control-oriented models are needed to enable optimal control in buildings. Learning mathematical models of buildings from sensor data has a fundamental property that the
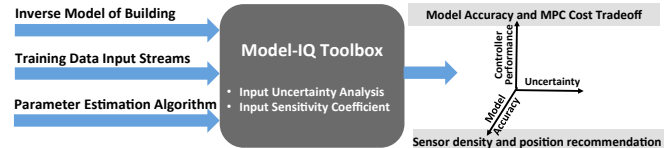
Figure 1: Model-IQ Toolbox uncertainty analysis for building controls.

model can only be as accurate and reliable as the data on which it was trained. Any measurement exhibits some difference between the measured value and the true value and, therefore, has an associated uncertainty. Non-uniform measurement conditions, limited sensor calibration, the amount of sensor data and the amount of excitation of the plant make the measurements in the field vulnerable to errors. In the case of using sensor data for training inverse models (e.g., grey box or black box), the goal is to provide maximum benefit, in terms of model accuracy, for the least sensor cost.

Small and medium sized buildings constitute more than 90% of the commercial buildings stock, but only about 10% of such buildings are equipped with a building automation system [11]. A proposed approach to obtaining the necessary data for generating a high-fidelity building models involves installing temporary sensors and measuring the necessary model inputs and outputs to enable training and testing of the building model. A recent report by the Department of Energy (DoE)[4] also emphasizes a program focused on adapting wireless sensor technology into an inexpensive system for energy-efficiency optimization of selected zones in commercial buildings. Therefore, there is economic value in performing an uncertainty analysis for such installations in order to better assess the tradeoffs involved in sensor installation cost and building performance.

However, a major challenge to the use of models for buildings controls lies in understanding the impact of uncertainty in the model structure, the estimation algorithm, and the quality of the training data. It is known that the quality of the training data, characterized by uncertainty, depends on factors such as the accuracy of sensors, sensor placement and density, and the assumption that air is well mixed. It is intuitive to assume that installing additional sensors to obtain higher quality training data should result in more accurate models, which will further result in better performance of a model based controller (e.g., Model Predictive Control (MPC)). However an understanding of the cost-benefit associated with adding additional sensors to a building is either limited or missing altogether. The reason for this is twofold:

a) It is not clear how the quality of the data from sensors affects the accuracy of a building model. This is because

data quality is only one of several factors that may affect model accuracy.

b) It is hard to analytically establish the effect of model accuracy on the performance of a model based closed-loop controller for buildings.

The goal of this paper is to study the cost-benefit effect of adding temporary low cost wireless sensors to a zone to improve model accuracy and subsequently enable low-cost implementation of advanced control schemes such as Model Predictive Control (MPC) (see Fig. 1). We first perform an input uncertainty analysis to classify the effect of the quality of training data on the accuracy of a "grey-box" building inverse model. We show how additional sensors can affect the training data quality. We empirically evaluate the tradeoff between model accuracy and MPC performance, i.e., all things being the same, for different model accuracies how MPC performance varies. This paper has the following contributions:

1. Model-IQ, a methodology for offline assessment of training data quality versus model accuracy, is presented. This scheme can be used to rank training inputs which affect the model accuracy the most.

2. A simulation based approach to study the influence of model accuracy on the performance of MPC for buildings is also presented.

3. The inferences from (1) and (2) allow us to formulate the trade-off between additional sensor cost and model accuracy for *real buildings* based on measurement data. Fig. 1 provides an overview of Model-IQ, available as an open-source toolbox for uncertainty propagation analysis in CPS with model-based control systems.

1.1 Sources for Uncertainty in Modeling

Uncertainty in modeling the dynamics of the underlying physical system is largely due to (a) the model structure, (b) the performance of the parameter estimation algorithm and (c) the uncertainty in the training data. In this effort, we assume the first two are fixed and focus on understanding the effect of uncertainty of the training data from the building and environment sensors on the overall performance of a model-based controller for the buildings' HVAC systems.

The uncertainty in training data can be characterized in two ways: bias error or random error. Biases are essentially offsets in the observations from the true values. Bias error can also be referred to as the systematic error, precision or fixed error. The bias in the sensor measurement is due to a combination of two reasons. The first reason is the sensor precision. The best corrective action in this case is to ascertain the extent of the bias (using the data-sheet or by re-calibration) and to correct the observations accordingly. The sensor may also exhibit bias due to its placement, especially if it is measuring a physical quantity which has a spatial distribution, e.g., air temperature in a zone. In this case, it is hard to detect or estimate the bias unless additional spatially distributed measurements are obtained. Random error is an error due to the unpredictable (e.g., measurement noise) and unknown extraneous conditions that can cause the sensor reading to take some random values distributed about a mean.

The density and location of sensors in a zone affect the deviation of the measured value from the true value. For in-

stance, a zone thermostat sensor placed too close to the wall, window, supply or return air duct can introduce a bias in the zone temperature measurement. A bias in the zone temperature value can lead to wastage of energy and discomfort with simple zone air control schemes like On-Off and PID control. Both the controllers are *model-independent* i.e., they only used the measurement of the *process variable* (which is the room temperature in this case) to compute the control signal that will either track the set-point (PID) or keep the temperature bounded around the set-point (On-Off). As we proceed to apply *model-based control* schemes for building retrofits, the bias or the uncertainty in the measured data will also influence the accuracy of the model itself which in turn affects the performance of the model based controller, which is the focus of this paper.

Organization: This paper is structured as follows. We begin with a short primer on the inverse modeling process for buildings in Section 2. The Model-IQ approach for input uncertainty analysis for inverse models is presented in Section 3. In Section 4, we quantify the effect of the model accuracy on the performance of a model predictive controller. Section 5 presents a data-driven case study in which we demonstrate our approach on sensor data obtained from a real building. Section 8 follows the related work with a discussion on the use of the free and open-source Model-IQ toolbox.

2. INVERSE MODELING FOR BUILDINGS

The main objective of an HVAC system for air temperature control is to reject disturbances due to outside weather condition and internal heat gain caused by occupants, lighting and plug-in appliances. Therefore, the building model must accurately capture the thermal response of the building to the different disturbances. In an inverse model, the parameters of the model can be estimated or tuned from actual measurements and the variables of the model can be, subsequently, predicted. Building models can be broadly classified into three categories:

1. *White-box* models are based on the laws of physics and permit accurate and microscopic modeling of the building system. High fidelity building simulation programs like EnergyPlus and TRNSYS [7] fall into this category. Although such models provide a high degree of accuracy they are unsuitable for control design due to their high level of complexity and a large number of parameters. Furthermore, the process of constructing the model and tuning the parameters with limited data is very time consuming and not cost effective.

2. *Black-box models* are not based on physical behaviors of the system but rely on the available data to identify the model structure. These models are often purely statistical and have a simple structure (e.g., linear regression). However, they provide little insight into the dynamics dictating the system behavior.

3. *Grey-box models* fall in between the two above categories. A simplified model structure is chosen loosely based on the physics of the underlying system and the available data is used to estimate the values of the model parameters. These models are suitable for control design and still respect the physics of the system.
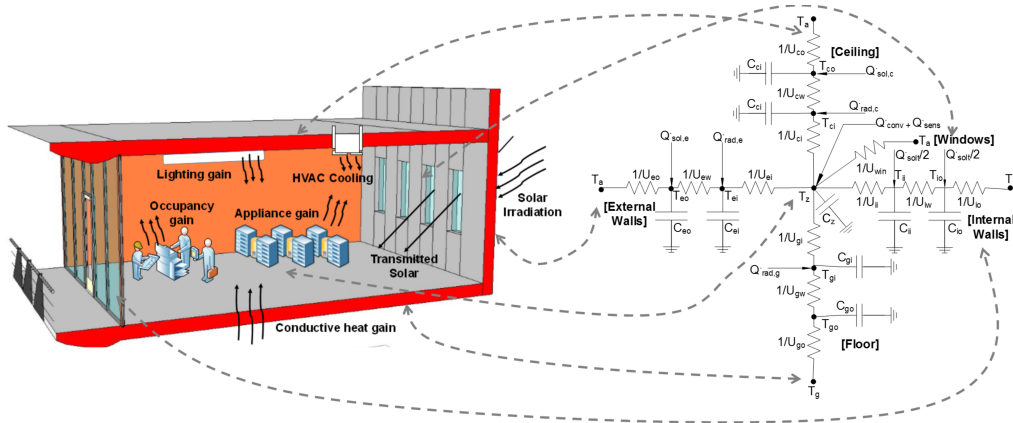
Figure 2: RC lumped-parameter model representation for a thermal zone obtained from information about the zone geometry and usage.

2.1 Model Structure

In this paper we will focus on the analysis of only grey-box models as they allow for balance between model fidelity and complexity. A commonly used grey-box representation of the thermal response of a building due to heat disturbances uses a lumped parameter Resistive-Capacitive (RC) network. This approach for modeling buildings effectively and efficiently represents the energy loss/storage and has been used widely, e.g., in [3, 15, 8]. Figure 2 shows an example of such a model for a single zone, as used in [3]. In this representation, the central node of the RC network represents the zone temperature $T_z(°C)$. The geometry of the zone is divided into different kinds of surfaces, each of which is modeled using a 'lumped-parameter' branch of the network. For instance, all the external walls of the zone are lumped into a single wall with 3R2C (3 resistances and 2 capacitance) parameters. The same process is applied to the ceiling, the floor and the internal (or adjacent) walls of the zone. The zone is subject to several (heat) disturbances which are applied at different nodes in the network in the following manner: (a) solar irradiation on the external wall $\dot{Q}_{sol,e}(\text{W})$ and the ceiling $\dot{Q}_{sol,c}(\text{W})$ is applied on the exterior node of the lumped wall, (b) incident solar radiation transmitted through the windows $\dot{Q}_{solt}(\text{W})$ is assumed to be absorbed by the internal and adjacent walls, (c) radiative internal heat gain $\dot{Q}_{rad}(\text{W})$ which is distributed with an even flux to the walls and the ceiling, (d) the convective internal heat gain $\dot{Q}_{conv}(\text{W})$ and the sensible cooling rate $\dot{Q}_{sens}(\text{W})$ is applied directly to the zone air, (e) the zone is also subject to heat gains due to the ambient temperature $T_a(°C)$, ground temperature $T_g(°C)$ and temperatures in other zones which are accounted for by adding boundary condition nodes to each branch of the network. The list of all parameters in the model is given in Table 1. Given this model, the nodal equations for the lumped external wall and the ceiling network are:

$$C_{eo}\dot{T}_{eo}(t) = U_{eo}(T_a(t) - T_{eo}(t)) + U_{ew}(T_{ei}(t) - T_{eo}(t)) + \dot{Q}_{sol,e}(t)$$
$$C_{ei}\dot{T}_{ei}(t) = U_{ew}(T_{eo}(t) - T_{ei}(t)) + U_{ei}(T_z(t) - T_{ei}(t)) + \dot{Q}_{rad,e}(t)$$
$$C_{co}\dot{T}_{co}(t) = U_{co}(T_a(t) - T_{co}(t)) + U_{cw}(T_{ci}(t) - T_{co}(t)) + \dot{Q}_{sol,c}(t)$$
$$C_{ci}\dot{T}_{ci}(t) = U_{cw}(T_{co}(t) - T_{ci}(t)) + U_{ci}(T_z(t) - T_{ci}(t)) + \dot{Q}_{rad,c}(t) \quad (1)$$

Similarly, one can write the equations for the dynamics of the nodes of the floor and internal wall network. The law of conservation of energy gives us the following heat balance equation for the zone

$$C_z\dot{T}_z(t) = U_{ei}(T_{ei}(t) - T_z(t)) + U_{ci}(T_{ci}(t) - T_z(t))$$
$$+ U_{ii}(T_{ii}(t) - T_z(t)) + U_{gi}(T_{gi}(t) - T_z(t))$$
$$+ U_{win}(T_a(t) - T_z(t)) + \dot{Q}_{conv}(t) + \dot{Q}_{sens}(t) \quad (2)$$

Differential equations in (1) and (2) can be combined to give a state space model of the system. Define $x = [T_{eo}, T_{ei}, T_{co}, T_{ci}, T_{go}, T_{gi}, T_{io}, T_{ii}, T_z]^T$ to be the state vector of all node temperatures. The input u is a vector of all the inputs to the systems, i.e., $u = [T_a, T_g, T_i, \dot{Q}_{sol,e}, \dot{Q}_{sol,c}, \dot{Q}_{rad,e}, \dot{Q}_{rad,c}, \dot{Q}_{rad,g}, \dot{Q}_{solt}, \dot{Q}_{conv}, \dot{Q}_{sens}]^T$.

The control input to the zone is the sensible cooling rate $\dot{Q}_{sens}$. The cooling rate can be controlled by changing the mass flow rate of cold air which enters the zone (in case of cooling) or by changing the set point of the supply air temperature. The rest of the inputs are disturbances to the zone. The elements of the system matrices depend nonlinearly on the U and C parameters. Let us consider $\theta = [U_{eo}, U_{ew}, \ldots, C_{ii}]^T$ as a vector of all the parameters of the model. Then the state space equations have the following representation which emphasizes the parameterization of the system matrices.

$$\dot{x}(t) = A_\theta x(t) + B_\theta u(t)$$
$$y(t) = C_\theta x(t) + D_\theta u(t) \quad (3)$$

The output matrix C_θ and the feed-forward matrix D_θ depend on the outputs of interest. For instance, if the output of the model is the zone temperature then $C_\theta = [0, 0, \ldots, 0, 1]$, which is a row vector with all entries equal to zero except the last entry corresponding to the zone temperature T_z equal to one. In this case $D_\theta = \mathbf{0}$, the null matrix.

This model structure is based on the underlying assumption that the air inside the zone is well mixed and hence it can be represented by a single node. Furthermore, only one-dimensional heat transfer is assumed for the walls and there is no lateral temperature difference. The parameters of the model are assumed to be time invariant.

Table 1: List of parameters

$U_{\star o}$	convection coefficient between the wall and outside air
$U_{\star w}$	conduction coefficient of the wall
$U_{\star i}$	convection coefficient between the wall and zone air
U_{win}	conduction coefficient of the window
$C_{\star\star}$	thermal capacitance of the wall
C_z	thermal capacity of zone z_i
g: floor; e: external wall; c: ceiling; i: internal wall	

2.2 Parameter Estimation (Model Training)

We discretize the continuous-time model in Eq. (3) with the measurement sampling time to obtain a discrete-time state space model:

$$x(k + 1) = \hat{A}_\theta x(k) + \hat{B}_\theta u(k)$$
$$y(k) = \hat{C}_\theta x(k) + \hat{D}_\theta u(k) \tag{4}$$

The goal of parameter estimation is to obtain estimates of the parameter vector θ of the model from input-output time series measurement data. The parameter search space is constrained both above and below by $\theta_l \leq \theta \leq \theta_u$. For a given parameter vector θ, the model, given by Eq. (4), can be used to generate a time series of the zone air temperature T_{z_θ} using the measured time series data for the inputs $u(k)$. The subscript θ denotes that the temperature value T_{z_θ} is the predicted value using the model with parameters θ and the inputs u. This model generated time series T_{z_θ} may then be compared with the corresponding observed values of the zone temperature T_{z_m}, and the difference between the two is quantified by a statistical metric. The metric usually chosen is the sum of the squares of the differences between the two time series. The parameter estimation problem is to find the parameters θ^*, subject to $\theta_l \leq \theta \leq \theta_u$, which result in the least square error between the predicted and the measured temperature values, i.e.,

$$\theta^* = \arg \min_{\theta_l \leq \theta \leq \theta_u} \sum_{k=1}^{N} (T_{z_m}(k) - T_{z_\theta}(k))^2 \tag{5}$$

where the summation is over the N data points of the input-output time series under investigation.

The least square optimization of Eq. (5) is a constrained minimization of a non-linear objective. It is solved using a trust region algorithm [6] like the Levenberg-Marquardt [16] algorithm. A well known problem with non-linear search algorithms is the problem of the solution getting stuck at a local minima. Furthermore, as opposed to black-box models, since the parameters of grey-box models usually have physical meanings, it is desirable that the initial parameter estimates θ_0 are as close as practicable to their (unknown) optimal (true) values. The initial values of the parameters can be estimated from the details of the constructions and materials used for the building.

3. MODEL-IQ

In this section, we describe the Model-IQ approach for analyzing uncertainty propagation for building inverse models. The accuracy of the building inverse model depends primarily on the following three factors:

(a) **The structure of the model** which depends on the extent to which the model respects the physics of the underlying physical system,

(b) **The performance of the estimation algorithm**. As discussed previously, in the case of non-linear estimation the performance of the algorithm depends heavily on the nominal values of the parameters, and

(c) **The quality of the training data**, which can be characterized by its uncertainty.

The main premise of the input uncertainty propagation is that once the model structure and the parameter algorithm are fixed,
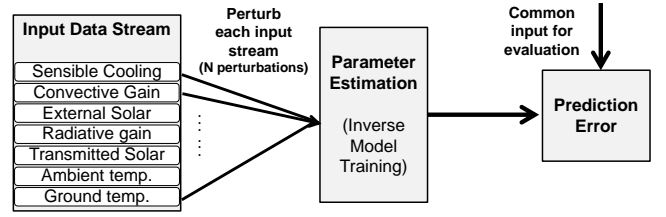

Figure 3: Overview of the Model-IQ input uncertainty analysis methodology, an offline method to confirm the influence of each training input on the accuracy of the model.

one can study the influence of the uncertainty in the training data on the accuracy of the model using virtual simulations which utilize artificial data-sets. Figure 3 shows an overview of the Model-IQ approach. We introduce an uncertainty bias in each of the training data streams in form of bounded perturbations around the unperturbed (nominal) values. This results in the creation of artificial training data sets each of which is similar to the original unperturbed data-set except for one input data stream. For each artificial data-set, we train a new inverse model and calculate its test error. A common test data set allows us to fairly compare the accuracy of the models in terms of their test root mean square error (RMSE). This allows us to quantify the effect of uncertainty bias in each input stream on the accuracy of the inverse model. For the remaining part of the section we describe the results of conducting the input uncertainty propagation analysis for a virtual building modeled in TRNSYS.

3.1 Inverse Model

The test-bed used for the input uncertainty analysis is a single zone building modeled in TRNSYS. The building is north facing, has 4 external brick walls each of which contains a large window, a concrete ceiling and a floor. For the simulation we use the `Philadelphia − TMY2` weather file which provides the ambient temperature and solar irradiation data for modeling. The building is assumed to be equipped with a HVAC system with a maximum cooling power of 3.5kW. In addition to the heat gains due to outside temperature and incident irradiation, the building is also subject to internal heat gains from occupants, appliances and lighting fixtures. Without lack of generality we only consider the case when the building is being cooled. The operation of the heating system would be similar.

The objective is to construct an inverse model for the thermal response of the building which can be used for model based control. A lumped parameter RC model was constructed for the building with a structure similar to the model explained in Section 2. The model contains 12 RC parameters which need to be estimated. The inverse model contains a total of seven inputs and an output. The six disturbance inputs are: the ambient temperature (T_a), the ground temperature (T_g), the external incident solar irradiation (Q_{sole}), the solar irradiation transmitted through the windows (Q_{soltr}), radiative heat gain (Q_{grad}) and convective internal heat gain (Q_{conv}). The output of the inverse model is the temperature of the zone while the control input is the sensible cooling rate (Q_{sen}). The training data for the model is in the form of time-series data for each of the inputs and the output. The training period is the month of June. The input-output time-series data is generated at a sampling rate of 2 minutes for the entire training
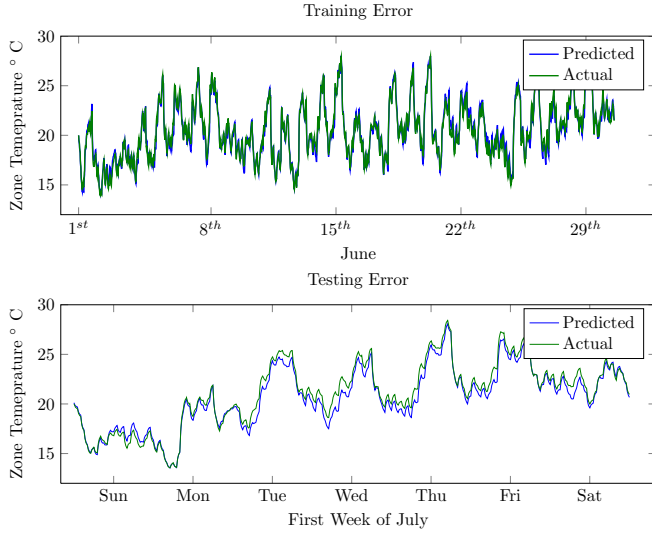
Figure 4: The fit between the predicted and actual values of the zone temperature for the training period in June (top figure) and for the testing period during the first week of July (bottom figure).

period.

For this case study, the nominal values of the RC parameters of the model were estimated from the construction details of the building, obtained from TRNSYS. Fig. 4 (top) shows the result of non-linear parameter estimation problem (5) for the training period of the state-space model. The comparison between the predicted zone temperature values from the model and the actual zone temperature is shown. The RMSE of the fit was 0.187 and the R^2 value is 0.971. The R^2 coefficient of determination is a statistical measure of the goodness of fit of a model. Its value lies between $[0, 1]$ with a value of 1 indicating that the model perfectly fits the data. The R^2 coefficient also indicates how much of the variance of the data can be described by the model. Measuring the fit on the training period alone is never sufficient, since the model may be over-fitting the data. Therefore, the accuracy of the inverse model was also tested on a test data-set. The test data-set corresponds to the first week of July. The time-series of inputs for the test period were used with the learned model and the results of the comparison between the predicted model output and the actual zone temperature is shown in Fig. 4 (bottom). The RMSE for the testing period was 0.292 with a R^2 value of 0.961. These stats are a better indicator of the accuracy of the model since during the testing period the model is subject to an input data-set that it was not trained on.

3.2 Input Uncertainty Analysis

The aim of this analysis is to determine the influence of bias in the training data inputs on the accuracy of the inverse model and then, to quantify the relative importance of the inputs. First, some notations are introduced for brevity. Consider a model with $m > 0$ input data sets given by $V = \{v_1, \cdots, v_m\}$. Note that these are inputs for model training, not the inputs for the model itself, e.g., although zone temperature is a model output, it is still a required data-set for model training. $V_{i,\delta} = \{v_i = v_i + \delta, v_j = v_j | i, j \leq m, j \neq i\}$ denotes the artificial data-set obtained by perturbing input u_i by an amount δ while keeping all other inputs data sets unperturbed. V_0 denotes the data-set in which all the inputs are unperturbed and is considered as the ground truth. Now, $\hat{M}_{V_{i,\delta}}$ is the inverse

model obtained by training on the data-set $V_{i,\delta}$ and $\hat{M}_{V_0}$ is the model obtained by training on a completely unperturbed data-set. The Model-IQ approach for conducting an input uncertainty analysis consists of the following steps:

(a) Establish a baseline (reference) model: The baseline model, $\hat{M}_{V_0}$, is the inverse model obtained by training on the unperturbed data set V_0.

(b) Determine which model outputs will be investigated for their accuracy and what are their practical implications.

(c) Each of the input data streams is then perturbed within some bounds. There are a total of P perturbations $\delta_1, \cdots, \delta_P$ for each input stream v_i. This results in N artificial data-sets $V_{i,\delta_1}, \cdots, V_{i,\delta_P}$ for each input stream i.

(d) For each perturbation, the inverse modeling process is run again and a new model $\hat{M}_{V_{i,\delta_k}}$ is obtained.

(e) The prediction accuracy of each of the trained model is evaluated on a common input data stream V_T. The accuracy of the model $\hat{M}_{V_{i,\delta_k}}$ is measured by the RMSE $r(\hat{M}_{V_{i,\delta_k}})$ between the predicted and the actual model output values for the common input stream V_T.

(f) Using the RMSE of the fit and the magnitude of the perturbation, determine the sensitivity coefficient for each input training stream.

For our case study, the baseline model is the model trained on unperturbed training data-set. The RMSE for the baseline model is denoted by $r(M_{V_0})$. The artificial data-sets are created in a normalized manner by adding (and subtracting) a bounded bias to the unperturbed data in the form of the per-cent change from the unperturbed (baseline) value i.e., the perturbations δ_k's are in form of per-cent changes around the unperturbed data point. Therefore, each data-point z_i belonging to the unperturbed input v_i gets perturbed to a new value of $\tilde{z}_i = z_i(1 + \delta_k/100)$. This is done so that every input is treated in the same manner regardless of the scale of the input. One can relate the per-cent change to the absolute value of the change, simply through the mean of the data-set. For example if the mean of unperturbed ambient temperature was 20°C, then the mean of data which was perturbed $\delta = +10\%$ would be 22°C which is equivalent to a mean absolute bias of 2° degrees in the ambient temperature. Each of the 7 training input data streams (Fig. 3) are perturbed one at a time within $[-20\%, 20\%]$ around the unperturbed nominal value with increments of 1%. Every perturbation for each of the inputs creates an artificial training set for the inverse model. Therefore for each of the 7 input streams, $N = 40$ additional artificial data-sets $V_{i,\delta_1}, \cdot, V_{i,\delta_{40}}$ were created resulting in a total 280 different training data-sets. The inverse model for the single zone building was trained on each of the artificial data-sets and the accuracy of the model was evaluated in terms of the RMSE on the test data-set. The use of a common test data-set for evaluating the accuracy of the model ensures a fairness in the comparison of the influence of the uncertainty among different inputs on the model accuracy.

Finally the model accuracy sensitivity coefficient is calculated as follows:

$$\gamma_i = \operatorname*{mean}_{k=1,\cdots,P} \left(\frac{(r(\hat{M}_{V_{i,\delta_k}}) - r(M_{V_0}))/r(M_{V_0})}{|\delta_k|} \right) \quad (6)$$
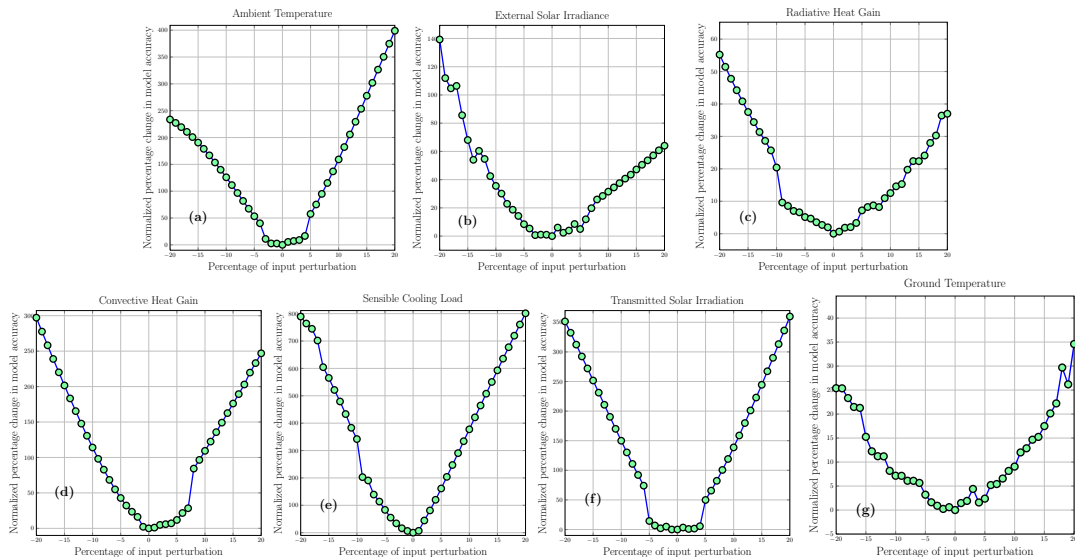
Figure 5: Input uncertainty analysis results for a single zone TRNSYS model. The x-axis shows the magnitude of the perturbation in percent change from the unperturbed data. The y-axis is the percent change in model accuracy wrt. the RMSE for the model trained on unperturbed data. Inputs shown: (a) ambient temperature (°C); (b) incident solar irradiation on the external walls (W); (c) radiative internal heat gain (W); (d) convective internal heat gain (W); (e) sensible cooling rate (W); (f) solar irradiation transmitted through the windows (W); and, (g) floor (ground) temperature (°C).

It is the mean of the ratio of the normalized change in the model accuracy to that of the normalized change in the magnitude of the input data stream. Both normalizations are with respect to the baseline case. The magnitude of the sensitivity coefficient γ_i can be interpreted as the mean value of the change in the RMSE of the model due to 1% bias uncertainty in the training data stream i. The sensitivity coefficient is sometimes also referred to as the influence coefficient or point elasticity. The results for the input uncertainty analysis for the TRNSYS building are shown in Fig. 5. These results align well with the intuition that as the magnitude of the uncertainty bias increases in the input data stream the inverse model becomes worse and its prediction error increases. This is the case for all the input data streams and it results in the parabolic trend. The shape of the curve varies from input to input, due to a different sensitivity coefficient value, and is an indicator of the extend to which a particular input influences the model accuracy.

The model accuracy sensitivity coefficients were calculated for every input data stream and their comparison is shown in Fig. 6. For the building under consideration, it is clear that the sensible cooling rate, ambient temperature, transmitted solar gain and convective heat gains should be measured accurately in order to learn a good inverse model. Although the results presented here assume a particular building and a specific model structure, the Model-IQ approach is general and works for any building inverse model.
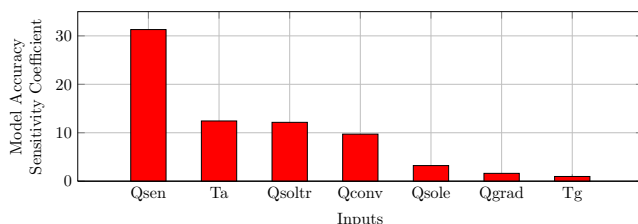
4. MODEL ACCURACY VS MPC PERFORMANCE

Input uncertainty analysis reveals important insights about the relationship between data quality and model accuracy. It is also necessary to examine if the model accuracy has any direct control performance impact, especially when energy-efficient control algorithms rely on the accuracy of the underlying mathematical model of the building in order to determine optimal control inputs. Installation of additional sensors in a building can yield better quality of data for model training. However there is a trade-off between the accuracy of an inverse model and the cost to obtain it. The trade-offs can be better understood if an end-to-end relationship between the data uncertainty, model accuracy and control performance are known. There is significant value in knowing how much the cost of a model predictive controller changes with the model accuracy. This information can be used to provide "target" accuracy levels for the inverse model, which in turn specify the degree of accuracy required on the sensing.

However, analytically determining the impact of the model accuracy on the MPC performance is a hard problem, due to the complexity of the model structure and the MPC formulation itself. For this reason, to quantify this effect we make use of an empirical analysis with the same single zone TRNSYS model used in Section 3. First, a model predictive controller was designed for the zone. The MPC simulation is then run for models of different accuracy and the outputs are compared to reveal the trend of the model accuracy's effect on the MPC cost. We now describe the MPC formulation followed by the results of this analysis.

4.1 MPC formualtion

The MPC formulation involves optimizing a cost function subject to the dynamics of the system and the constraints on the zone temperature, over a finite horizon of time. After an optimal sequence of control inputs are computed, the first input is applied, then at the next step the optimization is solved again as shown in Fig. 7.
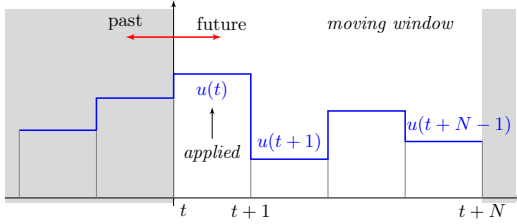

Figure 6: Model sensitivity coefficients for different input data streams.

Figure 7: Finite-horizon moving window of MPC: at time t, the MPC optimization problem is solved for a finite length window of N steps and the first control input $u(t)$ is applied; the window then recedes one step forward and the process is repeated at time $t + 1$.

The model in Eq. (4) can also be written as

$$x(k+1) = \hat{A}_\theta x(k) + \hat{B}_\theta u(k) + \hat{E}_\theta d(k)$$
$$y(k) = \hat{C}_\theta x(k) + \hat{D}_\theta u(k)$$

where the control input $u(k)$ is the cooling rate $\dot{Q}_{sens}$ to the zone, and $d(k)$ is the vector of all the disturbances to the zone (ambient temperature, heat gains, etc.). To reduce the number of optimization variables we use the move-blocking technique. During each move-blocking window of length l, the control u is held constant. So $u(0) = u(1) = \cdots = u(l-1)$, $u(l) = u(l+1) = \cdots = u(2l-1)$ and in general $u(il) = u(il+1) = \cdots = u((i+1)l-1)$, i.e., MPC re-optimizes at integral multiples of the window length il only.

Let us consider a control horizon H in terms of move-blocking windows, so the number of time steps is Hl. At time $t = il$, the MPC problem is to minimize

$$\sum_{k=0}^{H-1} \sum_{\sigma = t+kl}^{t+(k+1)l-1} \left(P_U(\sigma) u(k) + P_T(\sigma) \left(y(\sigma - y_{sp}(\sigma))^2 \right) \right)$$

subject to

$$x(t) = x_0$$
$$\begin{bmatrix} x(t+kl+1) \\ \vdots \\ x(t+(k+1)l) \end{bmatrix} = \mathrm{diag}(A) \begin{bmatrix} x(t+kl) \\ \vdots \\ x(t+(k+1)l-1) \end{bmatrix}$$
$$+ \mathrm{col}(B) u(k) + \mathrm{diag}(E) \begin{bmatrix} d(t+kl) \\ \vdots \\ d(t+(k+1)l-1) \end{bmatrix}$$
$$u_{min}(\sigma) \le u(k) \le u_{max}(\sigma)$$

where the last two constraints hold for all $k = 0, \ldots, H-1$ and $\sigma = t+kl, \ldots, t+(k+1)l-1$, $\mathrm{diag}(\cdot)$ represents a block diagonal matrix of appropriate dimensions, and $\mathrm{col}(B)$ is the column vector constructed by stacking the columns of matrix B. $P_U(\sigma)$ is the price of electricity at time σ and $P_T(\sigma)$ is the penalty for errors in tracking the desired zone temperature trajectory $y_{sp}(\sigma)$. Both the cost and penalty functions vary throughout the day, e.g., the price of electricity can be high during the peak hours of the day as compared to the off peak hours. Similarly, the temperature set-point can change during the day depending on the zone occupancy. Note that in our MPC formulation we only consider soft constraints on the zone temperature. The initial state of the system is x_0, while $u_{min}(\sigma)$ and $u_{max}(\sigma)$ are the lower and upper bounds on the cooling rate which can vary during the day to account for equipment schedules. In order to use the state space model (4) for MPC, we also need to design a state observer, which provides estimates $\hat{x}(k|k)$ of the state of the plant model at every
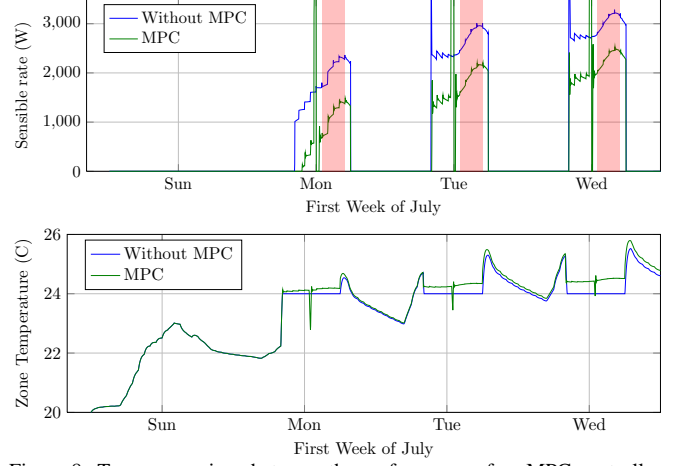

Figure 8: Top: comparison between the performance of an MPC controller with the default case without MPC. The peak-pricing period for each day is highlighted in red. Bottom: zone temperature values for both the controllers.

time step. The details of the state observer implementation can be viewed in the technical report [1].

4.2 Single zone example

The MPC described above was implemented for the single zone TRNSYS model. The cooling system of the building is always switched on during the occupancy period from 8 AM to 6 PM on weekdays and remains off during the weekend. The maximum and minimum constraints on the cooling rate were $u_{max} = 3500\,\mathrm{W}$ and $u_{min} = 0\,\mathrm{W}$. The temperature set-point was kept at $24\,°\mathrm{C}$ for the occupancy period. The zone temperature is allowed to float during the weekend. The simulation was run for a part of the first week of July. The building is also subject to peak demand pricing: the price of electricity is 10 times the nominal price during the on-peak hours, which are from 1 PM to 5 PM. We compare two different cases. The first is the comparison of the building operation with and without an MPC controller. Without MPC control, the cooling switches on at 8 AM and then tries to supply exactly the amount of cooling energy required to keep the temperature at $24\,°\mathrm{C}$ for the occupancy period. The total energy consumption for the simulation period is $93.71\,\mathrm{kW\,h}$. In this case, the power consumption remains high even during the peak pricing hours, resulting in a total cost of 511.83 units.

The baseline model for MPC is the model with the best RMSE (0.187) for the testing data. This model was trained on unperturbed data and was also used as the baseline for the input uncertainty analysis. The move-blocking step of MPC is 10 minutes and the MPC horizon is 2 hours. Figure 8 compares the performance of the MPC controller and the case without MPC. The MPC controller rapidly pre-cools the zone just before the peak pricing period begins (regions shown in red in Fig. 8). This can be seen in both the cooling rate and the zone temperature plots. Consequently, the energy consumption during the peak hours is reduced, which results in an overall lower energy cost. The total energy consumption for this case was $87.29\,\mathrm{kW\,h}$ and the total energy cost was reduced to 442.06 units. So there is a 13.63% reduction in the energy cost and a 6.85% reduction in the total energy consumption. The primary reason for the reduction in cost is the pre-cooling of the zone, which shifted part of the cooling demand from on-peak hours to off-peak hours. Another reason for the lower energy consumption is that because the
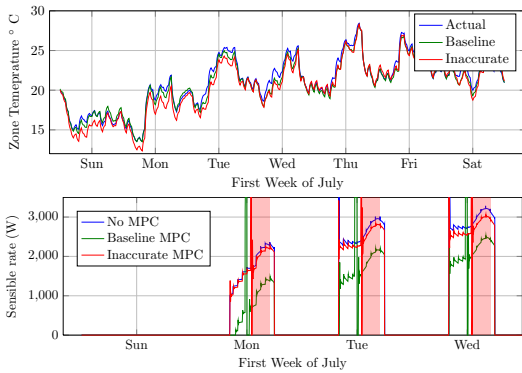
Figure 9: Top: comparison of the fit on the test data between the baseline model RMSE (0.187) and an inaccurate model (RMSE 0.538). Bottom: comparison between the MPC performance of the models. The red-regions indicated the peak pricing period for the day.

MPC has soft temperature constraints, the zone temperature is slightly above the temperature set-point, requiring it to use less cooling energy.

Having implemented MPC for the baseline model, we now use models trained on perturbed data and compare their performance with the baseline case. This allows us to observe the trend between MPC performance and model accuracy. An example of such a simulation run is shown in Fig. 9, which compares the baseline model with a relatively inaccurate model (with a much higher RMSE of 0.538 compared to 0.187 for the baseline model). Obviously an inaccurate model performs poorly compared to the "good" baseline case. The total energy consumption was 91.68 kW h, a 2.2% saving from the case without MPC. The total energy cost was 492.53 units, only 3.77% reduction compared to 13.63% for the baseline case. Several inverse models with different degrees of accuracy, in terms of their testing RMSE, were run with the MPC controller. Their savings, measured against the case when no MPC was used, are shown in Fig. 10. The trend of the plot aligns with intuition and shows that MPC performance deteriorates as the underlying model becomes less accurate. It can also be seen that the potential savings of MPC deteriorates quite rapidly as the model accuracy decreases (i.e., test RMSE increases). In the left region of the plot there is a positive cost benefit associated with adding additional sensors to improve the model accuracy from RMSE of 0.331 to 0.187. However, if the model accuracy is in the right region of the plot then there is no cost benefit associated with adding additional sensors to obtain improved models upto a certain RMSE threshold (0.331), beyond which the MPC savings are significant.

We have seen that models can lose their predictive performance if they are trained on uncertain (biased) data. The input uncertainty analysis reveals the extent to which different inputs are responsible for the accuracy of the inverse model. By empirically establishing a relationship between model accuracy and MPC performance, one can take informed decisions about the investment on additional sensors and the associated
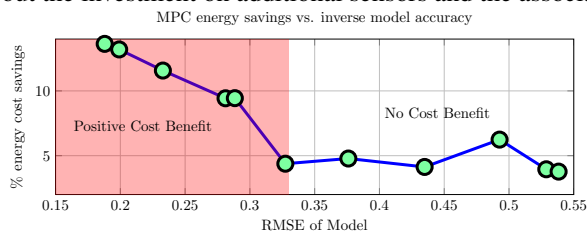

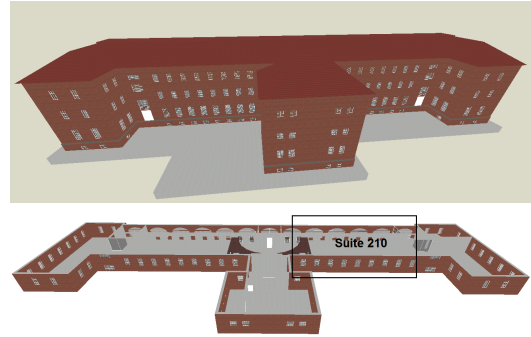Figure 10: MPC performance for models of different degrees of accuracy.

cost benefit for improving the data quality. In the next section we apply the Model-IQ toolbox on a model for a real building using real sensor data.

5. CASE STUDY WITH REAL DATA

In this section we present the results of applying the Model-IQ approach, described in Section 3, to real sensor data. First, we calculate the bias in the input data due to sensor placement. We then perform an input uncertainty analysis on the training data and the building inverse model.

The site chosen for analysis is called Building 101. Building 101, located in the Navy Yard in Philadelphia, is the temporary headquarters of the U.S. Department of Energy's Energy Efficient Building Hub [20]. It is a highly instrumented commercial building where the acquired data is continuously stored and is made available to Hub researchers. The building (see Fig. 11, top), is comprised of offices, a lunchroom, mechanical spaces, and miscellaneous spaces. For the case study, we focus on suite 210, a large office space on the second floor of the north-wing of the building as shown in Fig. 11 (bottom). This zone has a single external wall on the east side with 8 windows, a large interior wall on the west side which is adjacent to the porch area on the north-wing and two more adjacent walls on the north and the south side. In July 2013, functional tests were run from 00:00, 20-07-2013 to 22:29, 20-07-2013, on the air handling unit serving suite 210 as a part of an ongoing Hub project. During a functional test, the supply air temperature is changed rapidly so there is enough thermal excitation in the zone to generate a rich data-set for learning its dynamical model.

5.1 Sensor Placement and Data Quality

We first show how the location of the sensor effects the quality of measured data. We compared the thermostat measurement of suite 210 in building 101 with the mean of several temperature measurements made in the same zone but at different locations. A single point temperature measurement of a zone is based on the assumption that the air inside the zone is well mixed. The aim of our experiment was to analyze temperature data from suite 210 and determine if there is any location bias in the thermostat reading. The true value of the temperature of a zone (air volume) is extremely hard to determine. A better approximation of the true zone temperature is mean of temperature measurements taken from sensors which are uniformly located in the zone. Suite 210 at building 101 contains several sensors which log air temperature at different locations int he zone. The layout of the zone and the location of

Figure 11: 3D view of Building 101, the site chosen for the case study and the location of suite 210 in the north-wing of the building.
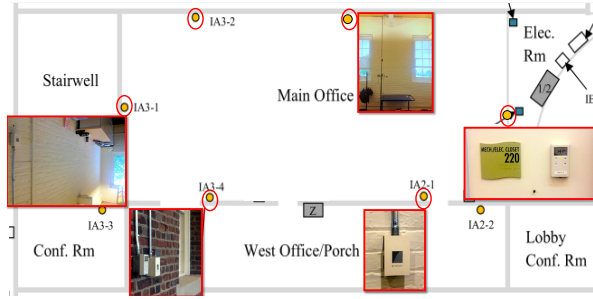
Figure 12: Temperature sensor locations for suite 210. The thermostat is located on the right wall. The location of 4 IAQ temperature data loggers and the portable temperature sensor cart is also shown.
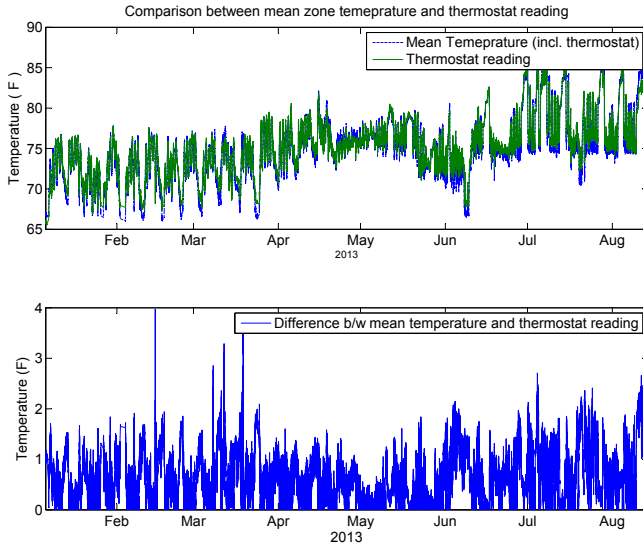

Figure 13: Comparison of thermostat reading and the mean temperature reading for suite 210. The bottom figure plots residuals between the two data-sets.

the temperature sensors is shown in Figure 12. There are a total of six different locations in the zone where air temperature is logged. The zone thermostat is placed on the south wall. There are 4 indoor air quality (IAQ) sensors which also measure zone temperature placed on the west, north and the east wall. An additional source of temperature measurement is a portable cart which measures temperatures at 8 different height levels. Since the different temperature sensors are located around the zone in a uniform manner, the mean of all the temperature measurements is a better representation of the zone temperature. The mean temperature value is compared with the thermostat measurement in Fig. 13. The values of the residuals are plotted. It can be seen that the difference between the thermostat and the mean temperature can be upto $4°F$. This suggests that the reading of the thermostat may be biased due to its location. The mean deviation in the temperature value is $0.71°F$ while the mean thermostat measurement is $75.8°F$ which is about 1% bias in the thermostat data. We will observe later that this can have a significant effect on the model accuracy for this zone. Another way to compare the two data-sets is through a scatter plot between the mean temperature and the thermostat reading. Figure 14 shows such a comparison along with a histogram plot for each axis. Two main inferences can be drawn form this plot. First, the spread of the data reveals how much the thermostat reading deviates from the mean temperature. A lower spread indicates that the two measurements are in agreement and that the well mixed

assumption holds well for the zone. Second, the histogram of the data-sets reveals that the thermostat data has a much larger variance that the mean temperature measurement.

5.2   Model-IQ implementation for Suite 210

We created the lumped parameter RC-network model for suite 210 using the principles described in Section 2. The model has 9 states, 9 inputs and 1 output. There are a total of 22 RC parameters in the model structure for this zone.

The temperature inputs to the model were the ambient temperature T_a(°C), boundary condition for the floor T_f(°C) given by the temperature of the zone on the first floor underneath suite 210, boundary condition for the ceiling T_c(°C) given by the temperature of the zone on the third floor above suite 210 and temperature of the adjacent porch area T_p(°C). The external solar irradiation Q_{sole} incident on the east wall is logged by a pyranometer. For the internal heat gain calculation, we consider 3 different heat sources: occupants, lighting and appliances. The number of people in the zone at different times during the functional test period was estimated using data from the people counter. We assume, using ISO standard 7730, that in a typical office environment the occupants are seated, involved in light activity and emit 75 (W) of total heat gain, 30% of which is convective and 70% is radiative gain. Using the power rating of the lighting fixtures and their efficiency, one can calculate the heat gain due to lighting. In this zone, lights contribute about 13 (W/m^2) with a $40\% - 60\%$ split between the convective and the radiative part. A constant heat gain due to the electrical appliances and computers is also assumed. The total internal convective heat gain Q_{conv} was obtained by adding the convective gain contributions from the three different heat gain sources. The total internal radiative heat gain was obtained in a similar way. The total internal radiative gain is further split into the radiative gain on the external wall Q_{qgrade} and the radiative gain on the ceiling Q_{qgradc} and applied as two separate inputs. The sensible cooling rate Q_{sen} was calculated using the temperature and mass flow rate measurements for the supply and the return air.

The sampling rate of the data was 1 minute. The total available data was split into a training set (80% of the data) and a test set (remaining 20% data). All the inputs for training the inverse model are shown in Figure 15. The output of the inverse model is the zone temperature T_z. After completion of the training process, the zone temperature predicted by the model is compared with the actual value of the zone temperature for both the training and the test period. The results of the
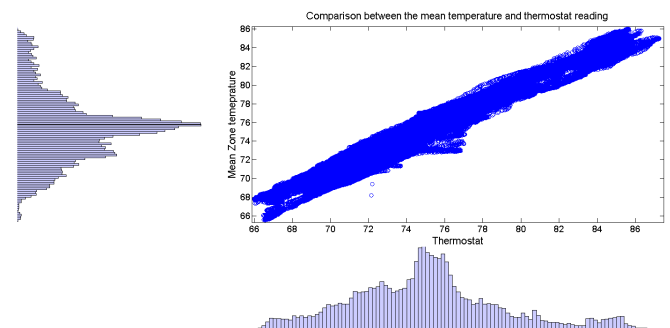

Figure 14: Scatter plot between the mean temperature measurement (y-axis) and the thermostat reading (x-axis). The spread of a data indicates the bias between the thermostat and the mean temperature measurement.
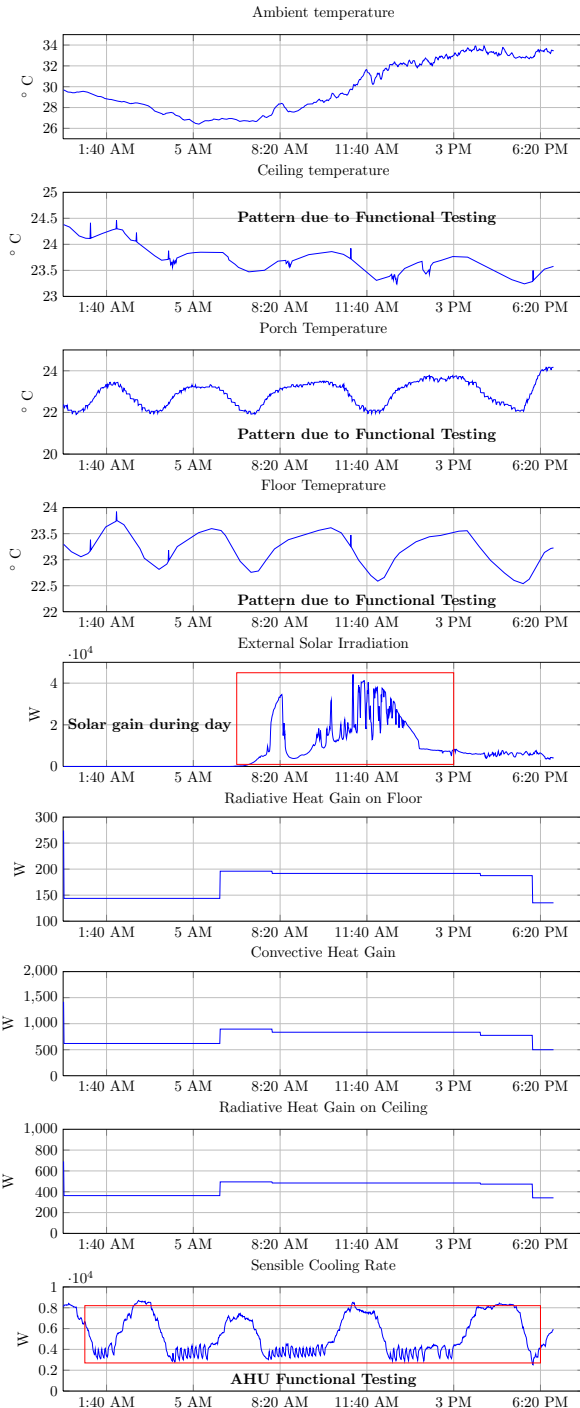
Figure 15: Training data for suite 210 of Building 101. The data obtained by running a functional test on the zone's air handling unit from 20-07-2013 00:00 to 20-07-2013 22:29

Figure 16: Fit between the predicted and actual zone temperature in suite 210. Top: for the training period, with RMSE = 0.062 and $R^2 = 0.983$. Bottom: for the test period with RMSE = 0.091 and $R^2 = 0.948$.

we also wanted to characterize the influence of uncertainty in the output of the model, the zone temperature, on the accuracy of the model. Therefore, in addition to the 9 aforementioned model inputs, perturbations were also introduced in the output training data-set i.e., in T_z. With 40 additional data-sets each, there were a total of 400 artificial data-sets. Each of these data-sets were used again for model training and the resulting model was evaluated for its accuracy in terms of the RMSE on the test-set.

5.3 Results

The results of the input uncertainty analysis for suite 210 in Building 101 are shown in Figure 17. Yet, again we see the parabolic trend obtained as a result of "artificial" uncertainty in the training data for each of the training data-sets. The sensitivity coefficients for the different training inputs were calculated. Figure 18 shows the comparison of the model accuracy sensitivity coefficients for the inverse model for suite 210. It is seen that the zone temperature has the largest model accuracy sensitivity coefficient suggesting that the accuracy of the model is quite sensitive to the zone temperature measurement. We saw in Section 5.1 that the thermostat measurement has an uncertainty bias of about 1%. From figure 17(j), we see that this can affect the model accuracy by upto 20%. This suggests that for this zone, it would be better to deploy additional low-cost wireless sensors just during the model training phase and get a better estimate of the zone temperature for training the inverse model. Also, the mean value obtained by adding more sensors could be used to re-calibrate or correct the thermostat reading for location bias, resulting in data which can yield an inverse model which can better represent the dynamics of the zone.

inverse model training are shown in Figure 16. The RMSE for the training data-set was 0.062 with R^2 equal to 0.983 (Figure 16, top) while the RMSE and R^2 values for the test set were 0.091 and 0.948 respectively (Figure 16, bottom).

After successfully training the inverse model, we conducted an input uncertainty analysis on the input-output training data-set as described in Section 3.2. The model trained on unperturbed data serves as the baseline model for the uncertainty analysis. Similar to the case of the single-zone TRNSYS model, we created artificial data-sets from the training data by perturbing each input data stream within $[-20\%, 20\%]$ of the unperturbed values in increments of 1%. For this case study,
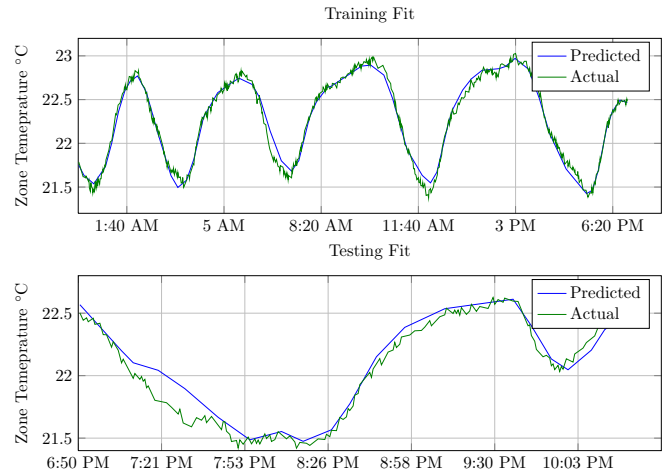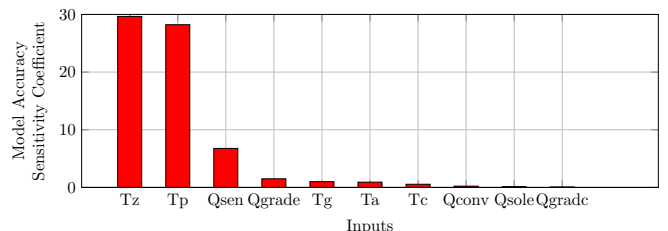

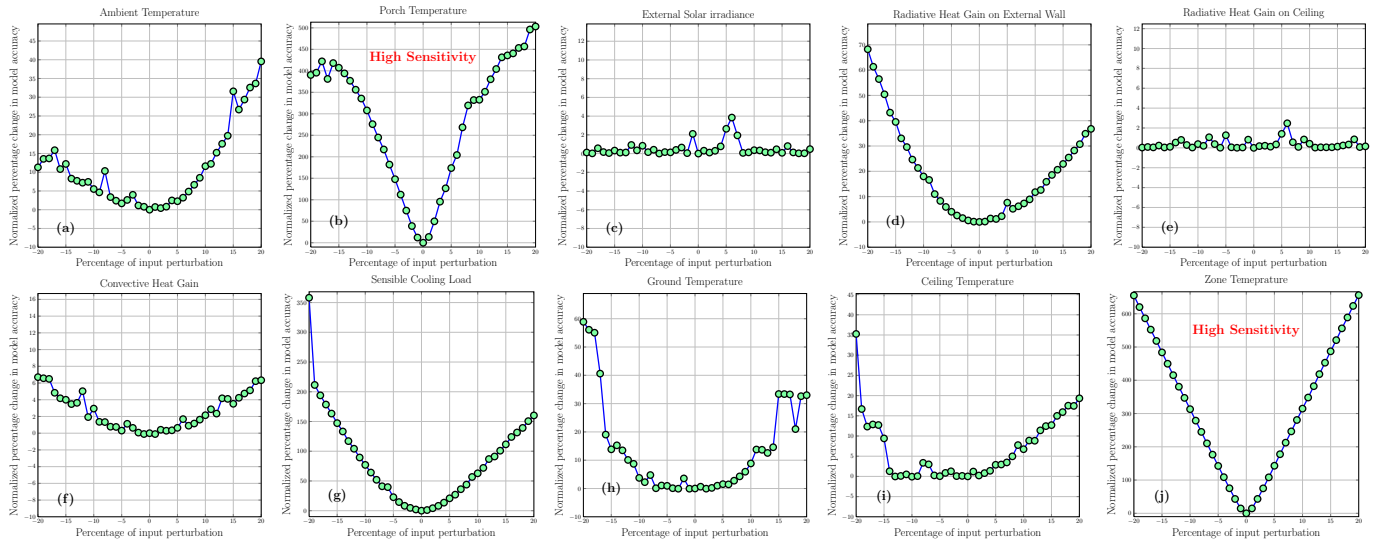Figure 18: Model accuracy sensitivity coefficients for Building 101

Figure 17: Input uncertainty analysis results for Building 101 inverse model. The x axis shows the magnitude of the perturbation in percent change from the unperturbed data while the y axis is the percent change in the model accuracy compared to the RMSE for the model trained on unperturbed data. The following inputs are shown: (a) ambient temperature (°C); (b) porch temperature (°C); (c) incident solar irradiation on the external walls (W); (d) and (e) radiative internal heat gain on external wall and ceiling (W); (f) convective internal heat gain (W); (g) sensible cooling rate (W); (h) floor temperature (°C); (i) ceiling temperature (°C), and (j) zone temperature (°C)

6. RELATED WORK

6.1 Model predictive control related

The treatment and analysis of the implementation of model based control schemes like MPC and optimal control for buildings have been very thorough. [10, 14] describe the implementation of MPC for energy efficient operation of buildings, supported by strong case studies. In [17] the authors consider uncertainty in the prediction of disturbances and propose a stochastic version of MPC. In [12], a reduced order model has been used for MPC. [18] advocates the use of simpler building models based on the physical description of the building. The authors highlight the building modeling process as a crucial part for building predictive control.

6.2 Sensitivity analysis related

Parametric sensitivity analysis of a model reveals the important parameters of the model which most significantly affect the model output. In [13], important input design parameters are identified and analyzed from points of view of annual building energy consumption, peak design loads and building load profiles. In [9], the authors extend traditional sensitivity analysis and increase the size of analysis by studying the influence of about 1000 parameters.

6.3 Uncertainty related

It is only recently in [2, 5] and [19], that researchers have analyzed the uncertainty in modeling for close loop control. In [2], the authors acknowledge that the performance of advanced control algorithms depends on the estimation accuracy of the parameters of the model. They design an MPC algorithm using a control model that is structurally identical to the plant model but has perturbed parameters. The closed loop system is simulated and the impact of the parameter perturbations on the energy cost is evaluated. Although, this methodology bears some similarity with the Model-IQ approach, there are some key differences. First, for a fixed model structure, the model parameters can change either due to the estimation process or due to the quality of data. The

cause of the parameter change has not been addressed in their work. So although one can identify which parameters should be estimated well, it is not clear how can one get a good estimate for that parameter. Second, the use of the same model as the control and the plant model is debatable. Realistically, the control model can only be an approximation of the plant dynamics but can never be exactly the same as the plant model. Which is why we used the TRNSYS building as the plant model in our MPC simulation to make it more realistic. In [5], the authors discuss the development of a control-oriented simplified modeling strategy for MPC in buildings using virtual simulations. [19] presents a methodology to automate building model calibration and uncertainty quantification using large scale parallel simulation runs. The method considers global sensitivity analysis using probabilistic data while we consider a fixed bias error.

7. DISCUSSION AND LIMITATIONS

(a) *Scalability*: Although the Model-IQ approach has been presented for the case of a single zone, it can be easily extended for a multi-zone scenario in which zones interact with each other. One method of dealing with this case is to treat the neighboring zone as a boundary condition (temperature node) for the zone of interest. We saw this in the example of the input uncertainty analysis for Suite 210, in the case study in Section 5, where the porch area was an adjacent zone and its temperature was a boundary condition for our zone model.

(b) *Measurement process*: The accuracy of the model is affected by the sampling rate and the quantity of data. It is necessary that the model is re-tuned or re-trained as the operating conditions of the building change or due to seasonal changes. Problems of optimal experimentation design for building inverse models, minimum frequency of model re-tuning and minimum duration of training period are of interest and will be investigated as part of future work.

(c) *Sensor placement*: Using real data we have shown an example of how sensor placement can result in a bias in its measurement. However, we do not directly map the sensor

placement/density to the bias.

Model-IQ Toolbox: The Model-IQ methodology has been implemented into an open-source toolbox. As shown in Fig. 1, the toolbox takes the building inverse model, an estimation algorithm and the training data set as input. The toolbox runs user specified input-output uncertainty analysis and compares the model accuracy sensitivity coefficients to identify the important input training data streams.

8. CONCLUSION

We introduced Model-IQ, a methodology and a toolbox for analysis of uncertainty propagation for building inverse modeling and controls. Given a plant model and real input data, Model-IQ automatically evaluates the effect of the uncertainty propagation from sensor data to model accuracy to controller performance. Through analysis with a high fidelity virtual building modeled in TRNSYS and a case study with real measurements from an office building, we show:

(a) Uncertainty bias present in the training input adversely effects the accuracy of the building inverse model. The extent of the influence of uncertainty in each training data stream on the model accuracy can be quantified through an input uncertainty analysis.

(b) We evaluate the relationship between model accuracy and performance of a MPC controller. Our empirical treatment of this analytically hard problem is both new and realistic compared to related work. We demonstrate that an accurate building inverse model can result in a MPC cost reduction of more than 13% while a bad model will barely reduce the cost (3%).

(c) We run the Model-IQ toolbox on a data-set obtained form a real building. We show that the density and placement of sensors are responsible for introducing a location based bias in the measured data. We observe that a bias of 1% degrades the model accuracy by 20%.

Model-IQ is a first step towards an automated tool to determine the minimum number of sensors, with their appropriate placement in the building, required to capture an adequate building model for model-based control strategies.

Acknowledgments

References

[1] M. Behl, T. X. Nghiem, and R. Mangharam. Uncertainty Propagation from Sensing to Modeling and Control in Buildings - Technical Report. Technical report, University of Pennsylvania, Oct 2013.

[2] S. Bengea, V. Adetola, K. Kang, M. J. Liba, D. Vrabie, R. Bitmead, and S. Narayanan. Parameter estimation of a building system model and impact of estimation error on closed-loop performance. In *CDC-ECC*, 2011.

[3] J. E. Braun and N. Chaturvedi. An inverse gray-box model for transient building load prediction. *HVAC and R Research*, 8(1), 2002.

[4] R. Butters, A. Schroeder, G. Hernandez, P. Fuhr, T. McIntyre, and W. Manges. US Department of Energy Advanced Sensing and Controls for Energy Efficient Buildings: A Cross Cutting Project. In *ACEEE Summer Study on Energy Efficiency in Industry*, 2011.

[5] J. A. Candanedo, V. R. Dehkordi, and P. Lopez. A control-oriented simplified building modelling strategy. In *13th Conf. Intl. Building Perf. Simulation Ass.*, 2013.

[6] T. F. Coleman and Y. Li. An Interior Trust Region Approach for Nonlinear Minimization Subject to Bounds. *SIAM Journal on optimization*, 6(2), 1996.

[7] D. B. Crawley, J. W. Hand, M. Kummert, and B. T. Griffith. Contrasting the Capabilities of Building Energy Performance Simulation Programs. *Building & Environment*, 43(4), 2008.

[8] T. Dewson, B. Day, and A. Irving. Least Squares Parameter Estimation of a Reduced Order Thermal Model of an Experimental Building. *Building and Environment*, 28(2), 1993.

[9] B. Eisenhower, Z. O'Neill, V. A. Fonoberov, and I. Mezić. Uncertainty and sensitivity decomposition of building energy models. *J. Building Perf. Simulation*, 5, 2012.

[10] D. Gyalistras, A. Fischlin, M. Morari, C. Jones, F. Oldewurtel, A. Parisio, F. Ullmann, C. Sagerschnig, and A. Gruner. Use of weather and occupancy forecasts for optimal building climate control. Technical report, Technical report, ETH Zürich, 2010.

[11] S. Katipamula et al. Small-and Medium-Sized Commercial Building Monitoring and Controls Needs: A Scoping Study. Technical report, Pacific Northwest National Laboratory (PNNL), 2012.

[12] D. Kim and J. E. Braun. Reduced-order building modeling for application to model-based predictive control. *SimBuild, National Conference of IBPSA-USA*, 2012.

[13] J. C. Lam and S. Hui. Sensitivity analysis of energy performance of office buildings. *Building & Environment*, 31, 1996.

[14] Y. Ma, F. Borrelli, B. Hencey, B. Coffey, S. Bengea, and P. Haves. Model Predictive Control for the Operation of Building Cooling Systems. *Control Systems Technology, IEEE Transactions on*, 20(3), 2012.

[15] T. L. McKinley and A. G. Alleyne. Identification of Building Model Parameters and Loads using On-site Data Logs. *Third National Conference of IBPSA-USA*, 2008.

[16] J. J. Moré. The levenberg-marquardt algorithm: implementation and theory. *Numerical analysis*, 1978.

[17] F. Oldewurtel, A. Parisio, C. Jones, M. Morari, D. Gyalistras, M. Gwerder, V. Stauch, B. Lehmann, and K. Wirth. Energy efficient building climate control using stochastic model predictive control and weather predictions. In *American Control Conference*, 2010.

[18] S. Prívara, J. Cigler, Z. Váňa, F. Oldewurtel, C. Sagerschnig, and E. Žáčeková. Building modeling as a crucial part for building predictive control. *Energy and Buildings*, 2012.

[19] S. N. Slaven Peles, Sunil Ahuja. Uncertainty quantification in energy efficient building performance simualtions. In *International High Performance Buildings Conference*, 2012.

[20] US Department of Energy. EEB Hub: Energy efficient buildings hub, 2013.